

Supporting Information

**High Conductivity Ag-Based Metal-Organic Complexes as
Dopant-Free Hole-Transport Materials for Perovskite Solar
Cells with High Fill Factor**

Yong Hua^{†a}, Bo Xu^{†a}, Peng Liu^b, Hong Chen^a, Haining Tian^d, Ming Cheng^a, Lars
Kloo^b, Licheng Sun^{a, c, *}

^a Organic Chemistry, Center of Molecular Devices, Department of Chemistry, School of Chemical Science and Engineering, KTH Royal Institute of Technology, SE-10044, Stockholm, Sweden. Fax: (+46) 8-791-2333 E-mail: lichengs@kth.se

^b Applied Physical Chemistry, School of Chemical Science and Engineering, Department of Chemistry, KTH Royal Institute of Technology, Teknikringen 30, SE-100 44, Stockholm, Sweden

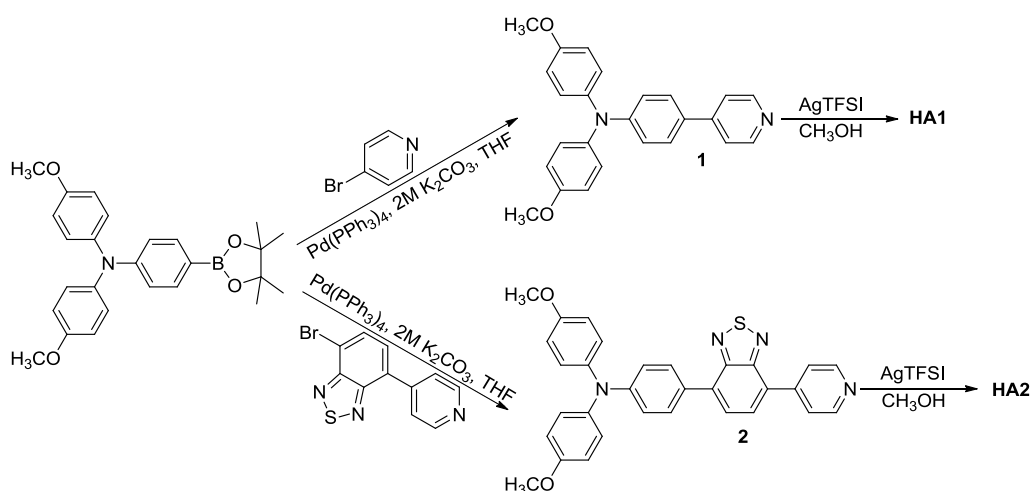
^c State Key Laboratory of Fine Chemicals, DUT-KTH Joint Research Centre on Molecular Devices, Dalian University of Technology (DUT), 116024 Dalian, China

^d Physical Chemistry, Department of Chemistry-Ångström Laboratory, Uppsala University (UU), SE-751 20 Uppsala, Sweden.

Experimental Section

Materials and Reagents

4-methoxy-N-(4-methoxyphenyl)-N-(4-(4,4,5,5-tetramethyl-1,3,2-dioxaborolan-2-yl)phenyl)aniline¹ and 4-bromo-7-(pyridin-4-yl)benzo[*c*][1,2,5]thiadiazole² were synthesized according to literature methods. Silver bis(trifluoromethane-sulfonyl)imide (AgTFSI) and 4-bromopyridine were purchased from Sigma-Aldrich Company and used as received without further purification. Solvents and other chemicals were also commercial available. ¹H and ¹³C NMR spectra were recorded on a Bruker AVANCE 500 MHz spectrometer. SEM images were obtained from JEOL JSM-7401F operating at 2 kV. Time-resolved photoluminescence was performed by using a time-correlated single-photon counting (TCSPC) spectrometer. The excitation of the sample was carried out with a picosecond diode laser (Edinburgh Instrument, EPL470) at 470 nm. The synthetic routes of two HTMs **HA1** and **HA2** are outlined in Scheme S1 and the details are depicted.



Scheme S1. The synthesis routes of **HA1** and **HA2**

General procedures for the preparation of **1** and **2**.

The mixture of 4-bromopyridine or 4-bromo-7-(pyridin-4-yl)benzo[*c*][1,2,5]thiadiazole (1.00 mmol) and 4-methoxy-*N*-(4-methoxyphenyl)-*N*-(4-(4,4,5,5-tetramethyl-1,3,2-dioxaborolan-2-yl)phenyl)aniline (0.54 g, 1.25 mmol), Pd(PPh₃)₄ (100 mg, 0.016 mmol) and 2 N aqueous solution of K₂CO₃ (2 mL) in THF (20 mL) under N₂ atmosphere was heated to reflux for 12 h. Then the solvent was removed under vacuum and the residue was purified by column chromatography on silica gel using a 1:1 mixture of hexane and CH₂Cl₂ as eluent to afford the target compound.

4-methoxy-*N*-(4-methoxyphenyl)-*N*-(4-(pyridin-4-yl)phenyl)aniline (**1**)

A light yellow solid, 88%. ¹H NMR (400 MHz, CDCl₃, δ): 8.85 (d, *J* = 4.0 Hz, 2H), 7.98 (d, *J* = 4.0 Hz, 2H), 7.80 (d, *J* = 4.0 Hz, 2H), 7.15 (d, *J* = 4.0 Hz, 4H), 6.95 (d, *J* = 4.0 Hz, 2H), 6.83 (d, *J* = 4.0 Hz, 4H), 3.65 (s, 6H).

4-methoxy-*N*-(4-methoxyphenyl)-*N*-(4-(7-(pyridin-4-yl)benzo[*c*][1,2,5]thiadiazol-4-yl)phenyl)aniline (**2**)

A red solid, 85%. ¹H NMR (400 MHz, CDCl₃, δ): 8.87 (d, *J* = 4.0 Hz, 2H), 7.93 (d, *J* = 4.0 Hz, 2H), 7.80 (d, *J* = 4.0 Hz, 1H), 7.78 (d, *J* = 4.0 Hz, 1H), 7.15 (d, *J* = 4.0 Hz, 2H), 6.96 (d, *J* = 4.0 Hz, 2H), 6.74 (d, *J* = 4.0 Hz, 4H), 6.65 (d, *J* = 4.0 Hz, 4H), 3.65 (s, 6H).

General procedures for the preparation of HA1 and HA2.

A mixture of precursor **1** or **2** (2 mmol) and AgTFSI (1.25 mmol) in minimal ethanol was exposed to ultrasonic irradiation for two minutes. After filtration, the solid was washed with methanol for 3 times and dried under vacuum to yield the **HA1** and **HA2**.

HA1, a yellow powder. ^1H NMR (500 MHz, DMSO-*d*, δ): 8.56 (d, $J = 6.0$ Hz, 4H), 7.68 (d, $J = 6.0$ Hz, 4H), 7.67 (d, $J = 6.0$ Hz, 4H), 7.11 (d, $J = 6.0$ Hz, 8H), 6.97 (d, $J = 6.0$ Hz, 8H), 6.82 (d, $J = 6.0$ Hz, 4H), 3.76 (s, 12H). ^{13}C NMR (400 MHz, CDCl_3 , δ): 156.29, 150.38, 149.72, 147.02, 139.28, 127.56, 127.39, 126.95, 120.27, 118.20, 115.08, 55.25. HRMS (MALDI-TOF):, m/z : $[\text{M}^+]$ calcd for $\text{C}_{50}\text{H}_{44}\text{AgN}_4\text{O}_4$, 872.7700; found, 872.7745.

HA2, a dark red powder. ^1H NMR (500 MHz, DMSO-*d*, δ): 7.09-6.98 (m, 18H), 6.98-6.95 (m, 12H), 6.70 (d, $J = 4.0$ Hz, 2H), 6.63 (d, $J = 4.0$ Hz, 2H), 3.78 (s, 12H). ^{13}C NMR (400 MHz, CDCl_3 , δ): 156.14, 153.28, 152.97, 150.17, 148.92, 144.30, 139.53, 133.87, 130.04, 129.53, 127.59, 127.40, 127.20, 126.45, 123.48, 118.20, 115.05, 55.25. HRMS (MALDI-TOF):, m/z : $[\text{M}^+]$ calcd for $\text{C}_{62}\text{H}_{48}\text{AgN}_8\text{O}_4\text{S}_2$, 1141.0939; found, 1141.1006.

Electrochemical Measurements

Electrochemical experiments were performed with a CH Instruments electrochemical workstation (model 660A) using a conventional three-electrode electrochemical cell.

A glassy carbon electrode (diameter 3mm) was used as the working electrode, a platinum wire as the counter electrode, an Ag/AgNO₃ electrode as the reference electrode and 0.1 M of tetrabutylammoniumhexafluorophosphate (*n*-Bu₄NPF₆) in dichloromethane solution as supporting electrolyte. The cyclic voltammometric scan rate was 50 mV/s. Each measurement was calibrated with Fc. $E_{1/2}^{Fc} = 0.20$ V. $E_{HOMO} = -5.1 - (E_{1/2} - E_{1/2}^{Fc})$.

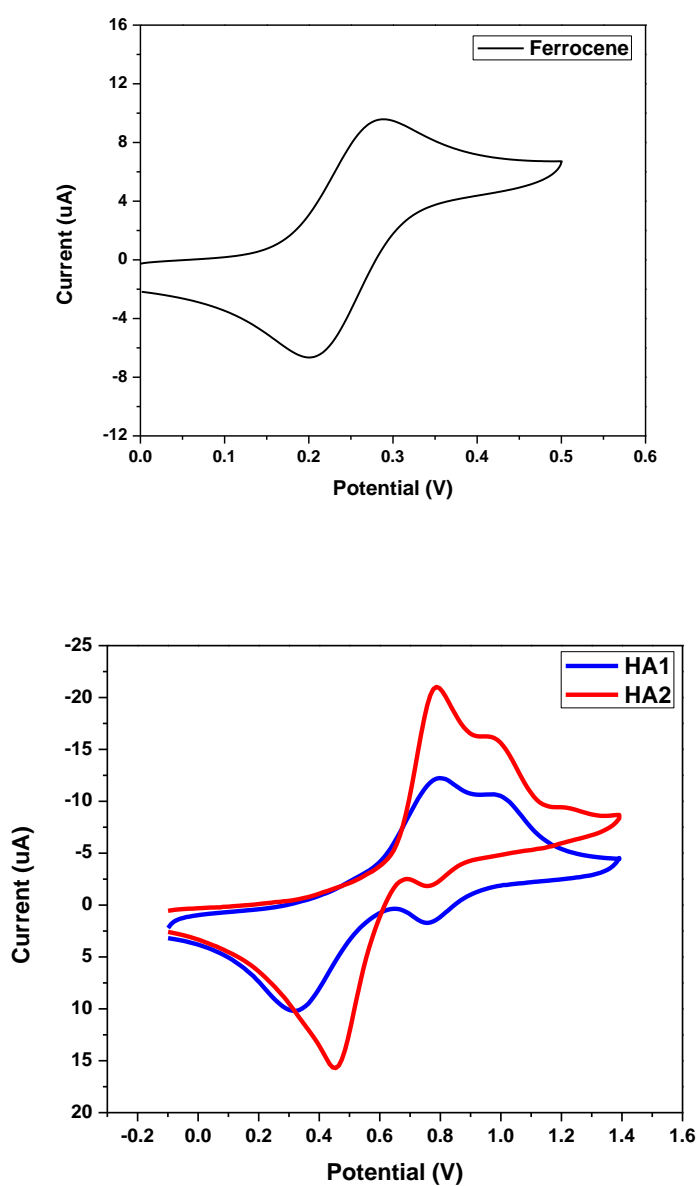


Figure S2. Cyclic voltammograms of Ferrocene, **HA1** and **HA2**.

Computational Details

In the simulation, Optimization and single point energy calculations are performed using the cam-B3LYP³ and the 6-31G** basis set for all atoms, without any symmetry constraints. All reported calculations were carried out by means of Gaussian 09.⁴

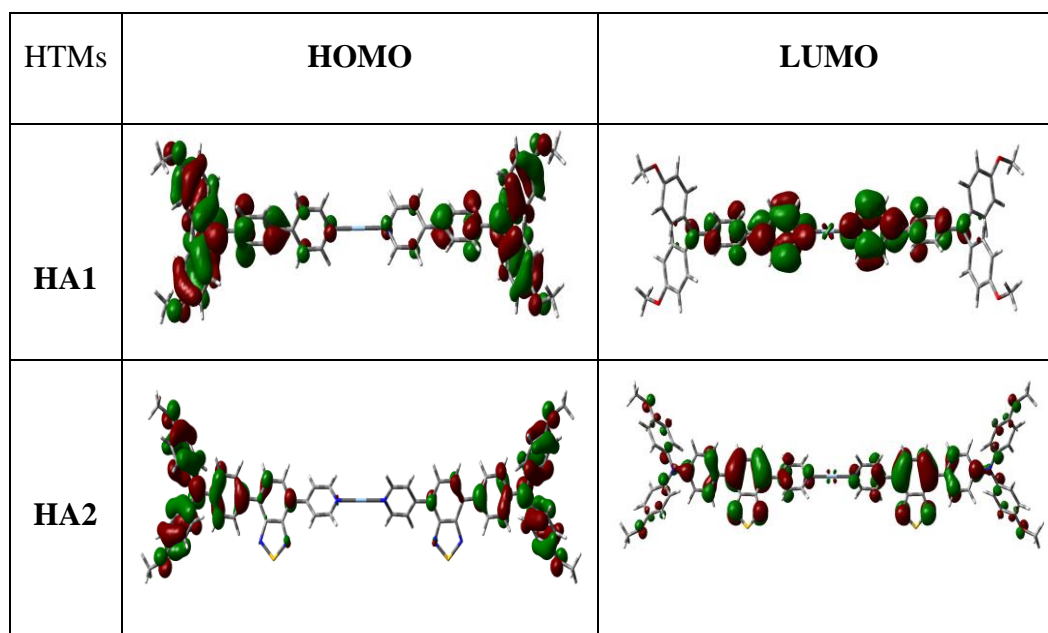


Figure S3. Frontier orbitals of HA1 and HA2.

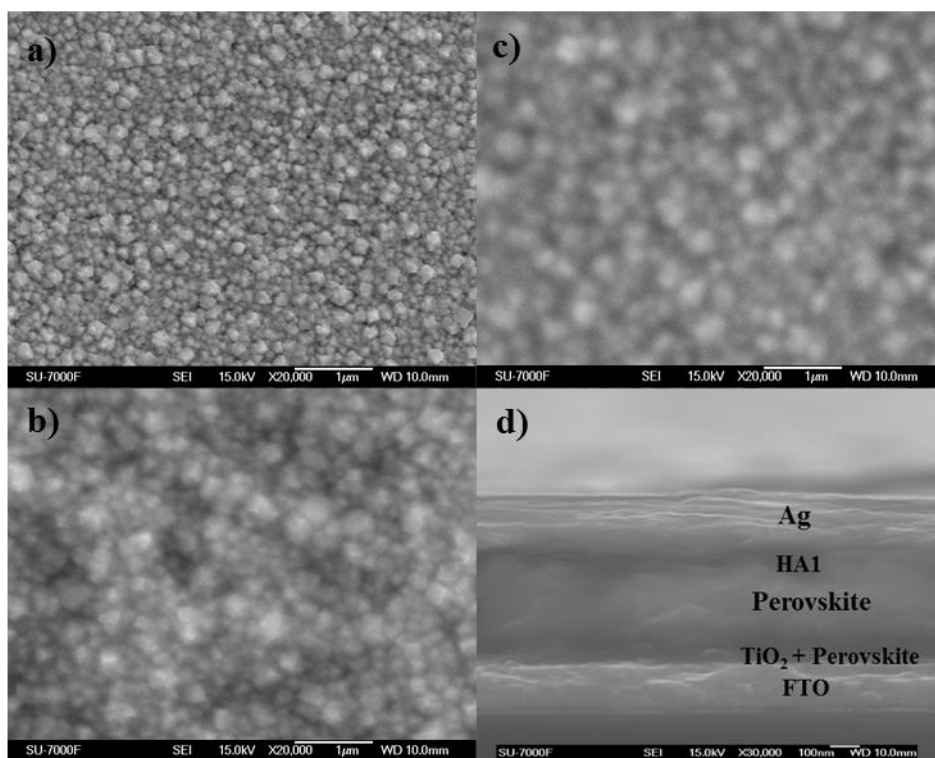


Figure S4, SEM images of perovskite (a), HA1 on the perovskite surface (b), Spiro-OMeTAD on the perovskite surface (c), Cross-sectional SEM images of devices of FTO/TiO₂/perovskite/HA1/Ag (d).

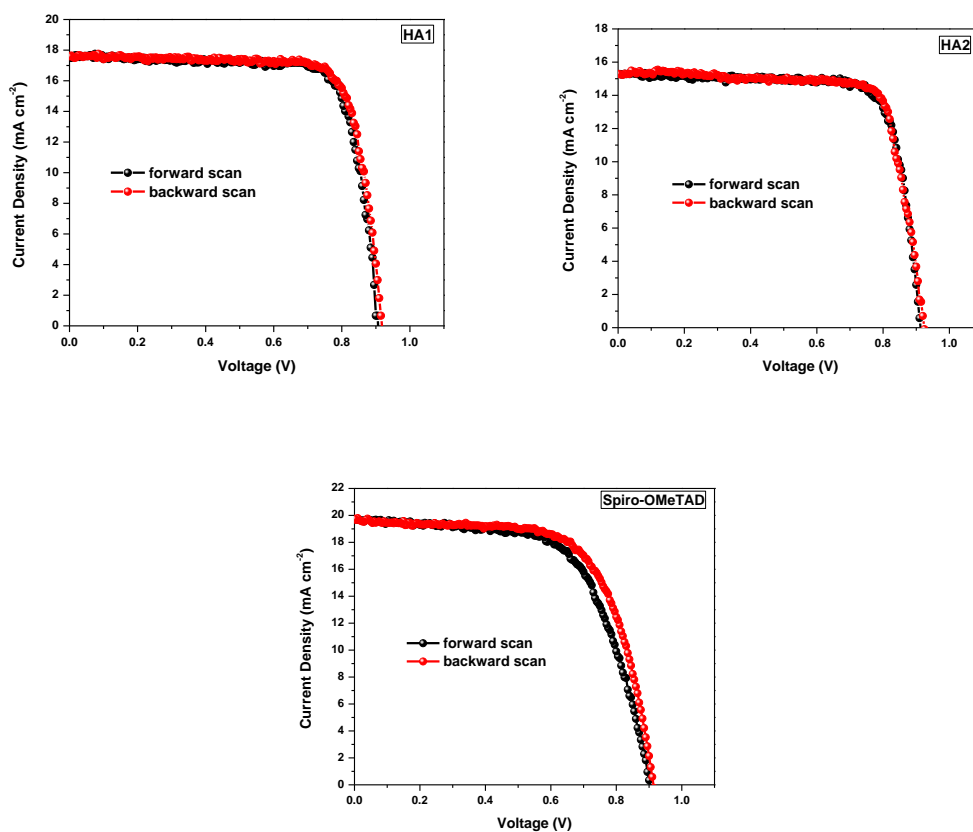


Figure S5. Perovskite solar cells employing various HTMs measured by forward and reverse scans, the curves were recorded at a scanning rate of 0.01 V s^{-1} .

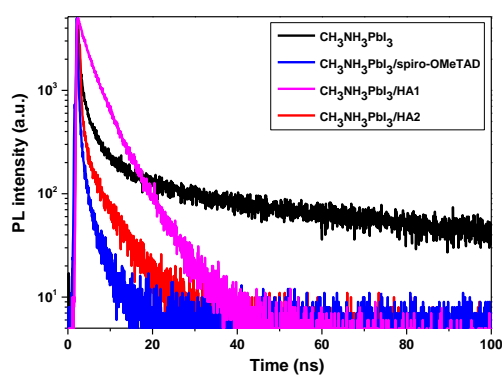


Figure S6. PL decay curves of bare $\text{CH}_3\text{NH}_3\text{PbI}_3$ and HTMs/ $\text{CH}_3\text{NH}_3\text{PbI}_3$ /glass devices.

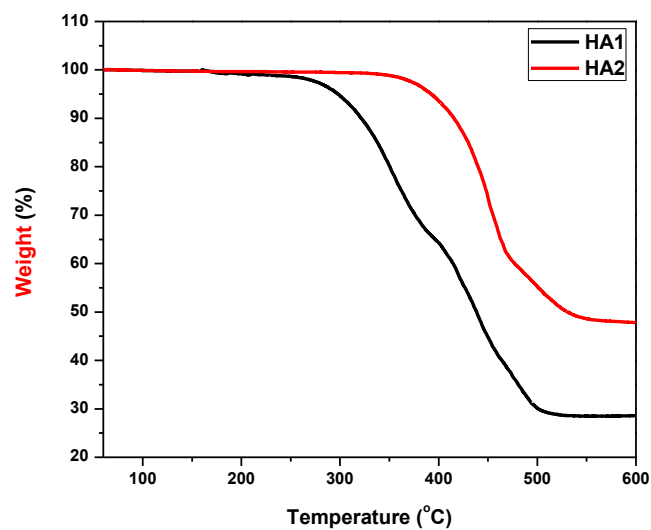


Figure S7. Thermogravimetric analysis of these two new HTMs.

Conductivity Measurement

The electrical conductivities of the HTMs films were determined by using two-probe electrical conductivity measurements, which were performed by following published procedure.^{4c} Conductivity devices structure was shown in Figure S8, and the electrical conductivity (σ) was calculated by using the following equation (1):

$$\sigma = \frac{W}{R L D} (1)$$

where L is the channel length 10 mm, W is the channel width 2 mm, D is the film thickness of the TiO_2 and HTM, and R is the film resistance calculated from the gradients of the curves.

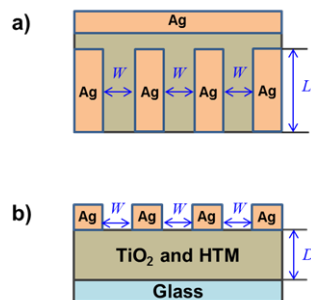


Figure S8. Schematic illustrations of the conductivity device: (a) top-sectional view; (b) cross-sectional view.

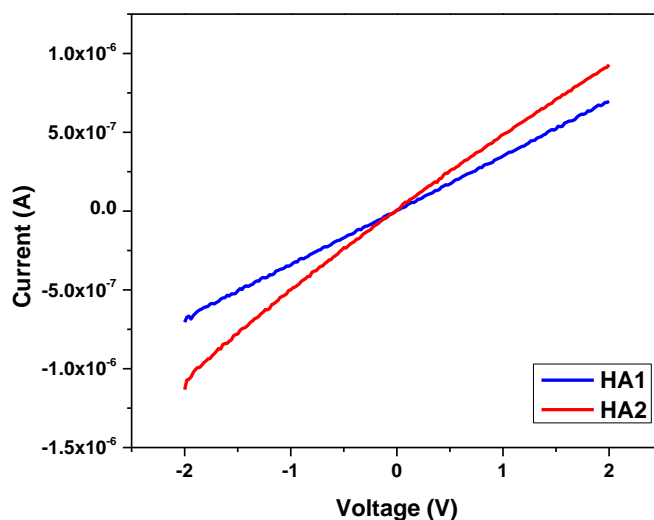


Figure S9. The original I-V data of conductivity measurement based on HA1 and HA2.

The conductivity devices were fabricated as following. Glass substrates without conductive layer were carefully cleaned in ultrasonic baths of detergents, deionized water, acetone and ethanol successively. A thin layer of nanoporous TiO_2 was coated on the glass substrates by spin-coating with a diluted TiO_2 paste (Dyesol DSL 18NR-T) with terpineol (1:3, mass ratio). The thickness of the film is ca. 500 nm, as

measured with a DekTakprofilometer. After sintering the TiO₂ film on a hotplate at 500 °C for 30 min, the film was cooled to room temperature. A solution of HTMs in chlorobenzene was subsequently deposited by spin-coating. Here the concentration of HA1 or HA2 is 20 mg mL⁻¹ in chlorobenzene. The doped spiro-OMeTAD/chlorobenzene (80 mg/mL) solution was prepared with addition of 20 μL Li-TFSI (520 mg Li-TFSI in 1 mL acetonitrile), and 30 μL tert-butylpyridine (tBP). Subsequently, a 200 nm thick Ag back contact was deposited onto the organic semiconductor by thermal evaporation in a vacuum chamber with a base pressure of about 10⁻⁶ bar, to complete the device fabrication. *J-V* characteristics were recorded on a Keithley 2400 semiconductor characterization system.

Mobility Measurements

Due to the low mobility of charge carriers in organic semiconductors, the injected carrier forms a space charge. This space charge creates a field that opposes the applied bias and thus decreases the voltage drop across junction; as a result, space charge limited currents (SCLCs) have been proposed as the dominant conduction mechanism in organic semiconductors by researchers. Mobility devices structure was shown in **Figure S10**, and ohmic conduction can be described by equations (2):

$$J = \frac{9}{8} \mu \epsilon_0 \epsilon_r \frac{V^2}{d^3} \quad (2)$$

where J is the current density, μ is the hole mobility, ϵ_o is the vacuum permittivity (8.85×10^{-12} F/m), ϵ_r is the dielectric constant of the material (normally taken to approach 3 for OSs), V is the applied bias, and d is the film thickness.

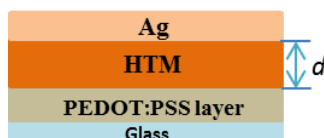


Figure S10. Schematic illustration of the mobility device.

Fluorine-doped tin-oxide (FTO) coated glass substrates (Pilkington TEC15) were patterned by etching with zinc powder and 2 M hydrochloric acid. The substrates were carefully cleaned in ultrasonic baths of detergents, deionized water, acetone and ethanol successively. The remaining organic residues were removed with 10 min by airbrush. A 40 nm thick PEDOT: PSS layer was spin-coated onto the substrates, which were then annealed at 120 °C for 30 min in air. The substrates were then transferred into a glove box for further fabrication steps. The HTMs were dissolved in anhydrous chlorobenzene. Here the concentration of HA1 or HA2 is 20 mg mL⁻¹ in chlorobenzene. The doped spiro-OMeTAD/chlorobenzene (80 mg/mL) solution was prepared with addition of 20 μ L Li-TFSI (520 mg Li-TFSI in 1 mL acetonitrile), and 30 μ L tert-butylpyridine (*t*BP). This HTMs solution was spin-coated at 3000 rpm to yield films. The thicknesses of the films are measured by using a Dektak 6M profilometer. 200 nm of silver was then evaporated onto the active layer under high vacuum (less than 10⁻⁶ mbar). J - V characteristics of the devices have been measured with a Keithley2400 Source-Measure unit, interfaced with a computer. Device

characterization was carried out in air.

Fabrication of perovskite solar cells

Fluorine-doped tin-oxide (FTO) coated glass substrates (Pilkington TEC15) were etched with zinc powder and 2 M hydrochloric acid. The substrates were carefully cleaned in ultrasonic baths of detergents, deionized water, acetone and ethanol subsequently. A thin compact TiO₂ blocking layer was deposited onto the FTO substrate by spray pyrolysis on a hotplate at 450 °C. A mesoporous TiO₂ film was deposited on the compact TiO₂ blocking layer by spin-coating at 6000 rpm for 45 s, using a commercial 20 nm TiO₂ paste (Dyesol 18NRT, Dyesol) diluted in 2-propanol (1:3, weight ratio), followed by annealing at 525 °C for 30 min, then cooling down to room temperature. PbI₂ in N,N-dimethylformamide solution (510 mg mL⁻¹) was stirred at 70 °C overnight. The PbI₂ solution was spin-coated on the mesoporous TiO₂ at 6000 rpm for 15 s and then dried at 100 °C for 15 min. After cooling down to the room temperature, the PbI₂ coated film was then dipped in the CH₃NH₃I solution (8.5 mg mL⁻¹ in 2-propanol) for 20 s. After the formation of the CH₃NH₃PbI₃, the film was rinsed at 70 °C for further manipulation. After cooling down to the room temperature, the doped or dopant-free HTMs solution was deposited by spin-coating at 3000 rpm for 30 s. Here the concentration of HA1 or HA2 is 20 mg mL⁻¹ in chlorobenzene. The doped spiro-OMeTAD/chlorobenzene (80 mg/mL) solution was prepared with addition of 20 μL Li-TFSI (520 mg Li-TFSI in 1 mL acetonitrile), and 30 μL tert-butylpyridine (*t*BP). Finally, 200 nm of silver was thermally evaporated on top of

the device to form the counter-electrode. The prepared PSCs samples were masked during the measurement with an aperture area of 0.126 cm² (diameter 4 mm) exposed under illumination.

[1] Y. Hua, L. T. L. Lee, C. S. Zhang, J. Z. Zhao, T. Chen, W. Y. Wong, W. K. Wong, X. J. Zhu, *J. Mater. Chem. A*, **2015**, 3, 13848-13855.

[2] I. Elguraish, K. L. Zhu, L. A. Hernandez, H. Amarne, J. W. Luo, V. N. Vukotica, S. J. Loeb, *Dalton Trans*, **2015**, 44, 898–902.

[3] A. D. Becke, *The Journal of Chemical Physics*.**1993**, 98, 1372.

[4] M. J. Frisch, G. W. Trucks, H. B. Schlegel, G. E. Scuseria, M. A. Robb, J. R. Cheeseman, G. Scalmani, V. Barone, B. M. a, G. A. Petersson, H. Nakatsuji, M. Caricato, X. L. and, H. P. Hratchian, A. F. Izmaylov, J. Bloino, G. Zheng, J. L. Sonnenberg, M. H. a. M. E. a. K. T. a. R. F. a. J. H. a. M. I. a. T. N. a. Y. H. a. O. K. and H. Nakai and T. Vreven and Montgomery, {Jr.}, J. A. and J. E. Peralta and F. Ogliaro and M. Bearpark and J. J. Heyd and E. Brothers and K. N. Kudin and V. N. Staroverov and R. Kobayashi and J. Normand and K. Raghavachari and A. Rendell and J. C. Burant and S. S. Iyengar and J. Tomasi and M. Cossi and N. Rega and J. M. Millam and M. Klene and J. E. Knox and J. B. Cross and V. Bakken and C. Adamo and J. Jaramillo and R. Gomperts and R. E. Stratmann and O. Yazyev and A. J. Austin and R. Cammi and C. Pomelli and J. W. Ochterski and R. L. Martin and K. Morokuma and V. G. Zakrzewski and G. A. Voth and P. Salvador and J. J. Dannenberg and S. Dapprich and A. D. Daniels and Ö. Farkas and J. B. Foresman and J. V. Ortiz and J. Cioslowski and D. J. Fox, Gaussian Inc. Wallingford CT **2009**.

[4] a)B. Xu, H. Tian, D. Bi, E. Gabrielsson, E. M. J. Johansson, G. Boschloo, A. Hagfeldt, L. Sun, *J. Mater. Chem. A*, **2013**,1, 14467-14470. b) B Xu, E. Sheibani, P. Liu, J. B. Zhang, H. N. Tian, N. Vlachopoulos, G. Boschloo, L. Kloo, Anders. Hagfeldt, L. C. Sun, *Adv. Mater.* **2014**, 26, 6629–6634. c) H. J. Snaith, M. Grätzel, *Appl. Phys. Lett.* **2006**, 89, 262114.